Ocean internal wave spectra inferred from seismic reflection transects

W. Steven Holbrook[1] and Ilker Fer[2]

[1] Internal waves affect many important dynamical processes in the ocean, but in situ observations of internal waves are infrequent and spatially sparse. Here we show that remote sensing of internal waves by marine seismic reflection methods can provide quantitative information on internal wave energy and its spatial variability at high lateral resolution and full ocean depth over large volumes of the ocean. Seismic images of the Norwegian Sea water column show reflections that capture snapshots of finestructure displacements due to internal waves. Horizontal wave number spectra derived from digitized reflection horizons in the open ocean compare favorably to the Garrett-Munk tow spectrum of oceanic internal wave displacements. Spectra within 10 km laterally and 200 m vertically of the continental slope show enhanced energy likely associated with internal wave-sloping boundary interactions. **Citation:** Holbrook, W. S., and I. Fer (2005), Ocean internal wave spectra inferred from seismic reflection transects, *Geophys. Res. Lett.*, *32*, L15604, doi:10.1029/2005GL023733.

1. Introduction

[2] Internal waves in the ocean develop when its stratification is disturbed. Internal waves play important roles in the ocean, including driving turbulence and diapycnal mixing [*Garrett*, 2003; *Ledwell et al.*, 2000; *Munk*, 1981; *Polzin et al.*, 1997; *Rudnick et al.*, 2003], affecting nutrient and biomass distribution [*Lennert-Cody and Franks*, 1999] and resuspending sediment [*Cacchione et al.*, 2002]. Two main sources for the internal-wave energy are internal tides originated by barotropic tidal flow over topography [*Baines*, 1982] and inertial waves generated in response to wind forcing [*Alford*, 2001]. In the open ocean, frequency- and wave number-domain representations of internal wave energy show a remarkably uniform energy spectrum and often adhere to the Garrett-Munk model spectrum [*Garrett and Munk*, 1975, 1979], which has a log-log slope indicating a power law near k^{-2}. This spectrum is thought to be maintained by a continual cascade of energy from lower to higher frequencies (and horizontal wave number) due to wave-wave interaction [*Müller et al.*, 1986; *Thorpe*, 1975]. Measurement of this energy spectrum typically requires in-situ time series measurements from moorings or towed instruments.

[3] In this paper we present a new method for quantifying internal wave energy in the ocean using acoustic imaging.

Recent work has shown that marine reflection seismology, a tool commonly employed to image the solid earth beneath the seafloor, can also produce detailed images of thermohaline finestructure in the ocean [*Holbrook et al.*, 2003]. The reflection method is remarkably sensitive to finestructure, imaging temperature contrasts as small as 0.04°C [*Nandi et al.*, 2004], produced by thermohaline intrusions [*Holbrook et al.*, 2003] and internal wave strains [*Nandi et al.*, 2004]. Here we show that seismic images of finestructure can quantify internal wave energy and its spatial variability by recording snapshots of finestructure displacements due to internal waves.

2. Data Acquisition and Processing

[4] Seismic data were acquired aboard R/V *Ewing* in September 2003. Sound energy was generated by a 6-element, 1340 cu. in. (22 liter) airgun array, fired at 37.5 m intervals, and recorded on a 6000 m, 480-channel hydrophone streamer. Hydrophone group spacing was 12.5 m, yielding a subsurface sampling interval of 6.25 m. Data were digitally recorded at a sample rate of 0.002 s. The ship traveled at 4.5 knots during acquisition. Seismic images were produced by standard processing techniques, including velocity analysis, moveout correction, stacking, and band-pass filtering (20–100 Hz). For the analysis presented in this paper, we processed data on Lines 30 and 32 (Figure 1).

[5] The seismic data were augmented by 110 expendable bathythermographs (XBT) and 12 expendable conductivity-temperature-depth probes (XCTD) deployed from the seismic vessel to produce a unique joint temperature/seismic data set, which provided information on the temperature and density finestructure associated with the reflections [*Nandi et al.*, 2004]. Buoyancy frequency profiles, $N(z) = [-g/\rho \, d\rho/dz]^{1/2}$, where z is depth, ρ is density, were calculated for all XCTD's (Figure 1).

3. Finestructure and Internal Wave Spectra

[6] Finestructure imaged in our data occurs dominantly in the boundary layer between the Norwegian Atlantic Current (NwAC) and underlying Norwegian Sea Deep Water (NSDW). Reflection patterns in the seismic image match water masses mapped by the XBT/XCTD survey [*Nandi et al.*, 2004]: an upper, variably reflective zone corresponds to the NwAC, which occupies the upper ~400 m; a lower non-reflective zone corresponds to the NSDW, which occupies ocean depths greater than ~600 m; and an intervening reflective zone corresponds to the boundary layer between the NwAC and the NSDW, where temperature decreases rapidly with depth from ~7°C to ~2°C. *Nandi et al.* [2004] showed that the seismically imaged finestructure has two causes: thermohaline intrusions, which follow isotherms,

[1] Department of Geology and Geophysics, University of Wyoming, Laramie, Wyoming, USA.
[2] Bjerknes Centre for Climate Research and Geophysical Institute, University of Bergen, Bergen, Norway.
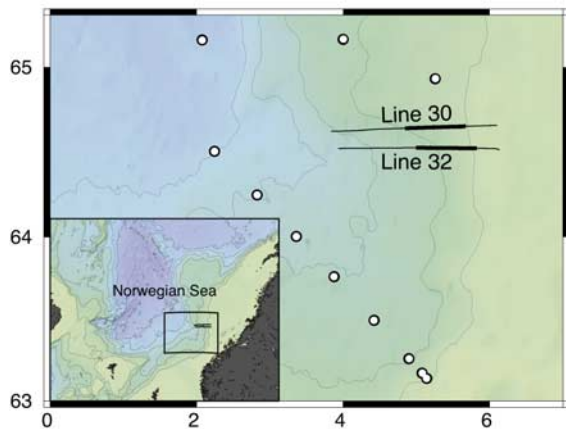
Figure 1. Location figure of the Norwegian Sea, showing seismic lines 30 and 32 and positions of expendable conductivity-temperature-depth (XCTD) probes (circles) used in this study. Bold lines show portions of seismic lines shown in Figure 2.

and internal wave strains, which cross isotherms. However, internal waves have another manifestation in the seismic images: all reflections undulate slightly, forming "sinusoidal" patterns with wavelengths from tens to thousands of meters and wave heights of tens of meters (Figure 2). Such undulations are ubiquitous in all ocean images our group has produced. They cannot be artifacts of processing (e.g., stacking velocity), as they are not observed on the seafloor or underlying geological reflections. Nor can they be a result of constructive/destructive interference patterns from thin layers, as the undulating reflections do not show the waveform and frequency variations that would be associated with tuning effects [*Widess*, 1973].

[7] The most straightforward interpretation of the observed undulations is that they represent deformation of finestructure by the ambient internal wave field. Irreversible finestructure in the ocean is known to be displaced by internal waves [*Gregg*, 1977], as has been acoustically imaged in the upper ocean with high-frequency echo sounders [*Proni and Apel*, 1975; *Stoughton et al.*, 1986]. We suggest that finestructure reflections represent "strain markers"; the seismic images represent acoustic snapshots that record displacements of those markers by internal waves. We test this assertion by calculating horizontal wave number spectra from the reflection displacements, ζ, and comparing them to the Garrett-Munk tow spectrum calculated following *Katz and Briscoe* [1979] (hereinafter referred to as GM76).

[8] Reflectors from isotherm-parallel finestructure were digitized at 6.25 m spacing (yellow lines, Figure 2) to calculate the horizontal wave number (k_x) power spectra of ζ (Figure 3). We used reflectors from two types of locations: open-ocean settings well above the seafloor, and zones of finestructure disruption within 10 km of the continental slope. Only reflectors that are roughly parallel to the reflective thermocline were selected for spectral analysis. (The thermocline is identified as the ~100-m-thick band of bright reflectance that demarcates a temperature

decrease from 7°C to 2°C [*Nandi et al.*, 2004].) Other reflectors that cross-cut the thermocline are clearly identifiable as reversible finestructure caused directly by internal wave strains [*Nandi et al.*, 2004] and were excluded from spectral analysis, which requires reflectors that are parallel to isopycnals. Reflectors were digitized on stacked sections using the "autotrack" feature in Paradigm's Focus® software, which selects the nearest peak (or trough) within a user-selected time gate (we used 8 ms) by tracking waveforms between a set of initial interpretive reflector picks. The resulting reflector picks were edited to remove cycle skips and converted to depth using a constant sound speed of 1480 m/s. Vertical displacements of reflectors are obtained by removing a straight line fit over the extent (typically ~5−30 km) of each reflector. Horizontal wave number spectra of vertical displacement were calculated with a Welch Fourier transform using half-overlapping Hanning windows of maximum 1024 points (6400 m). Ensemble-averaged spectra are calculated over about 178 km (open-ocean) and 30 km (near-slope) total length of reflectors and further band-averaged at $(\log_{10}k_x) = 0.1$ intervals. The spectra are scaled by the survey-average buoyancy frequency at the depth-range covered by the reflectors: N ~ 1.4 cph (1 cycle per hour = $2\pi/3600$ s^{-1}) in the open ocean at depths of 200−1000; N ~ 2.3 cph near the slope at depths of 200−600 m. Because the isopycnal displacements are vertically correlated, some ensembles of reflectors covering the same horizontal span but different depths are not independent. About one third of the open-ocean reflectors and half of the near-slope reflectors are deemed independent, and this is accounted for in the calculation of the confidence intervals presented in Figure 3.

[9] The resulting horizontal wave number spectra show a remarkable match to the GM76 tow spectrum (Figure 3). In both locations, the resulting power spectra are red and have a power-law slope close to −2 (Figure 3). For the open-ocean reflectors, the energy level agrees with GM76 within the confidence intervals for wavelengths >300 m and lies within a factor of 2 of GM76 down to wavelengths of ~30 m. This agreement with the stationary, horizontally isotropic deep-ocean internal wave model strongly supports our argument that the seismic images capture the internal wave field. Both observed spectra level off at around 30 cycles per km (~33 m), where noise begins to dominate. The noise in the spectra comes from high-k_x noise that is visible as "chop" in some digitized reflector shapes (Figure 2a) and is related to the signal level of the reflections; weaker reflections produce noisier spectral values at high wave numbers. However, because spectral levels are much lower at high k_x than at low k_x, even reflections with relatively low signal-to-noise can produce robust estimates of the total energy in the internal wave field over the wave number range shown in Figure 3.

[10] As the continental slope is approached, the reflection images show a marked change from smooth, continuous, gently undulating finestructure to more discontinuous, choppy finestructure that shows higher-amplitude undulations (Figure 2). These changes are reflected in the near-slope spectra, which show enhanced energy relative to the GM spectrum. This enhanced internal wave energy is likely associated with internal wave-sloping boundary interactions
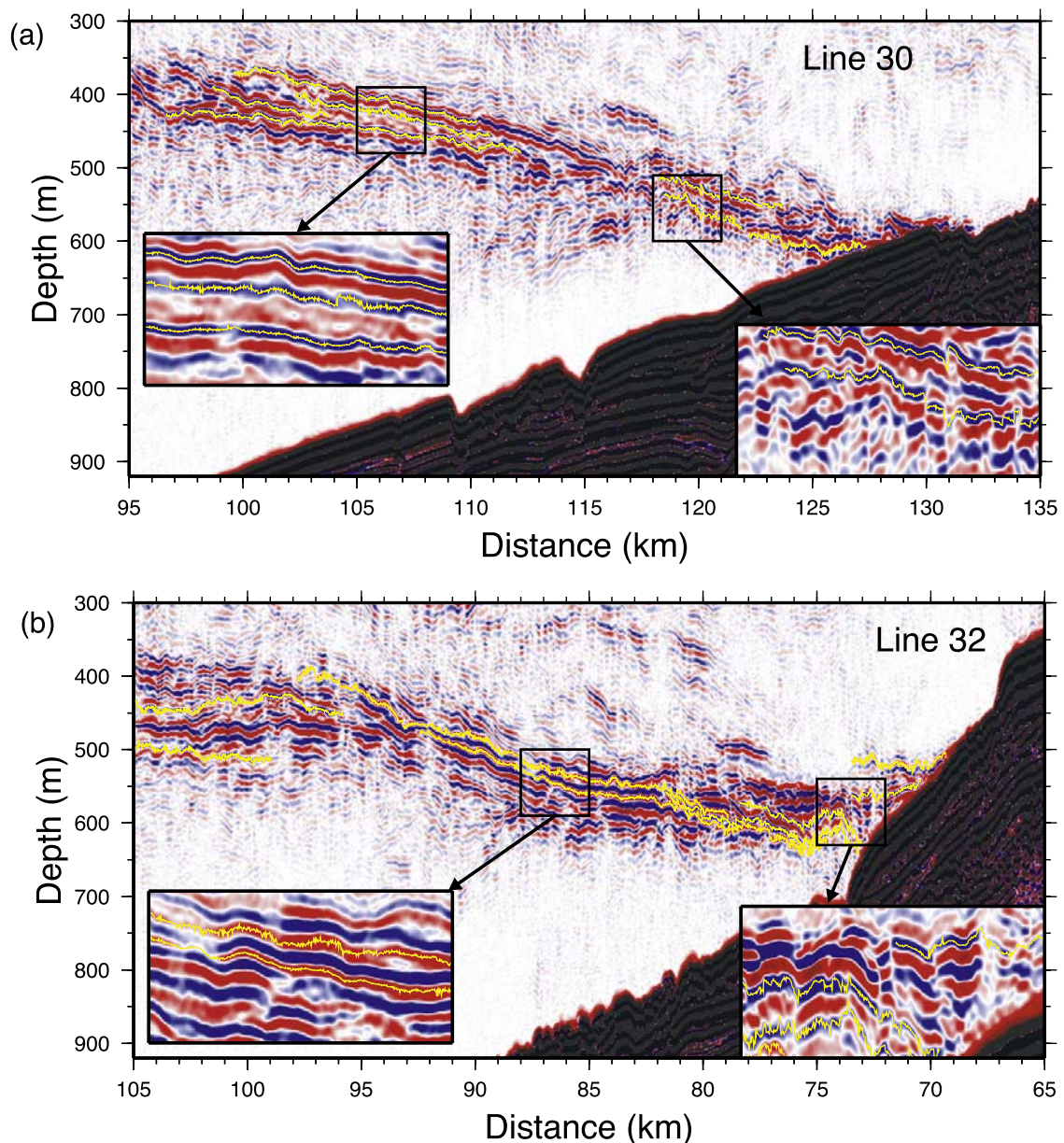
Figure 2. Seismic sections for Lines 30 and 32. Yellow lines show reflectors picked by "autotrack" algorithm for spectral analysis shown in Figure 3. Data are displayed so that peaks and troughs of reflections are red and blue, respectively, in the water column and grey and black in the solid earth. (a) Stacked seismic section of Line 30. The image shows a clear progression toward the slope from smooth, continuous finestructure (inset left) to highly disrupted finestructure (inset right). (b) Stacked seismic section of Line 32. As in Line 30, finestructure changes from smoothly undulating to more discontinuous as the continental slope is approached.

[*Eriksen*, 1985; *Gilbert and Garrett*, 1989; *Phillips*, 1977; *Thorpe*, 1987].

4. Discussion and Conclusions

[11] Our analysis demonstrates, and capitalizes on, the ability of reflection seismology to provide images of finestructure, and estimates of internal wave energy, with great lateral detail. The agreement between reflector-derived k_x spectra and the expected GM76 spectrum strongly supports our contention that the reflections faithfully capture vertical displacements of the internal wave field. Near the continental slope, k_x spectra show enhanced internal wave energy, which could be caused by wave reflection and generation processes at the sloping boundary [*Armi*, 1978; *Eriksen*, 1985; *Moum et al.*, 2002; *Nash et al.*, 2004; *Toole et al.*, 1994, 1997]. Here, there appears to be a change in spectral slope at around 3 cpkm after which the slope is close to that expected in the inertial-subrange of turbulence. The peak at this wave number, corresponding to a length scale of about 300 m, is likely the energy containing length scales feeding the cascade of energy into the inertial subrange. These
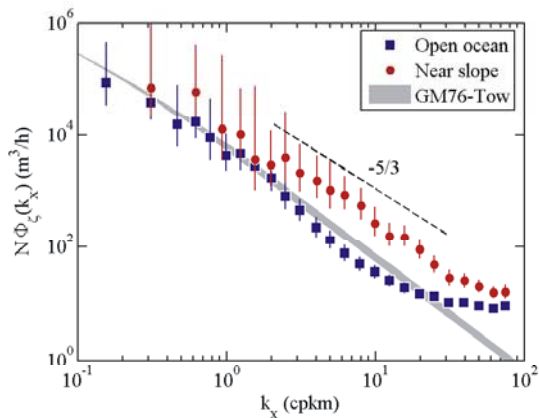
Figure 3. Horizontal wave number spectra of vertical displacement inferred from digitized reflectors from open ocean (squares), near slope (dots), all scaled by the average buoyancy frequency, N, covering the representative depth range of the chosen reflectors. Vertical bars are 95% confidence intervals. The GM76 tow spectrum is shown as a band for the observed range of $N = 1 - 2.5$ cph. The dashed line shows the $-5/3$ slope of the inertial subrange of turbulence, for reference.

observations suggest that seismic reflection images can provide important quantitative information on such processes as turbulence and boundary mixing.

[12] Our results imply that seismic reflection imaging constitutes an important new tool for remotely sensing and quantifying the internal wave field over large regions. The technique offers several unique advantages that can supplement the oceanographic measurements typically used to quantify the internal wave field: no other method is capable of imaging full ocean depths at such fine lateral detail. We suggest that ''seismic oceanography'' will be especially useful in quantifying the internal wave field when combined with more traditional measurements, such as time series from deep moorings, so that frequency and horizontal wave number spectra can be produced and compared. Such joint seismic/PO measurements could quantify and map regions of enhanced mixing and turbulence in great detail. With proper calibration, seismically determined wave number spectra from the extensive marine seismic data sets in existence can contribute significantly toward a global climatology of internal wave energy in the ocean.

References

Alford, M. H. (2001), Internal swell generation: The spatial distribution of energy flux from the wind to mixed layer near-inertial motions, *J. Phys. Oceanogr.*, *31*, 2359–2368.

Armi, L. (1978), Some evidence for boundary mixing in the deep ocean, *J. Geophys. Res.*, *83*, 1971–1979.

Baines, P. G. (1982), On internal tide generation models, *Deep Sea Res., Part A*, *29*, 307–338.

Cacchione, D. A., L. F. Pratson, and A. S. Ogston (2002), The shaping of continental slopes by internal tides, *Science*, *296*, 724–727.

Eriksen, C. C. (1985), Implications of ocean bottom reflection for internal wave spectra and mixing, *J. Phys. Oceanogr.*, *15*, 1145–1156.

Garrett, C. (2003), Internal tides and ocean mixing, *Science*, *301*, 1858–1859.

Garrett, C., and W. Munk (1975), Space-time scales of internal waves: Progress report, *J. Geophys. Res.*, *80*, 291–297.

Garrett, C., and W. Munk (1979), Internal waves in the ocean, *Annu. Rev. Fluid Mech.*, *11*, 339–369.

Gilbert, D., and C. Garrett (1989), Implications for ocean mixing of internal wave scattering off irregular topography, *J. Phys. Oceanogr.*, *19*, 1716–1729.

Gregg, M. C. (1977), A comparison of finestructure spectra from the main thermocline, *J. Phys. Oceanogr.*, *7*, 33–40.

Holbrook, W. S., P. Páramo, S. Pearse, and R. W. Schmitt (2003), Thermohaline fine structure in an oceanographic front from seismic reflection profiling, *Science*, *301*, 821–824.

Katz, E., and M. G. Briscoe (1979), Vertical coherence of the internal wave field from towed sensors, *J. Phys. Oceanogr.*, *9*, 518–530.

Ledwell, J. R., E. T. Montgomery, K. L. Polzin, L. C. St. Laurent, R. W. Schmitt, and J. M. Toole (2000), Evidence for enhanced mixing over rough topography in the abyssal ocean, *Nature*, *403*, 179–182.

Lennert-Cody, C. E., and P. J. S. Franks (1999), Plankton patchiness in high-frequency internal waves, *Mar. Ecol. Prog. Ser.*, *186*, 59–66.

Moum, J. N., D. R. Caldwell, J. D. Nash, and G. D. Gunderson (2002), Observations of boundary mixing over the continental slope, *J. Phys. Oceanogr.*, *32*, 2113–2130.

Müller, P., G. Holloway, F. Henyey, and N. Pomphrey (1986), Nonlinear interactions among internal gravity waves, *Rev. Geophys.*, *24*, 493–536.

Munk, W. (1981), Internal waves and small-scale mixing processes, in *Evolution of Physical Oceanography*, edited by B. A. Warren and C. Wunsch, pp. 264–290, MIT Press, Cambridge, Mass.

Nandi, P., W. S. Holbrook, S. Pearse, P. Páramo, and R. W. Schmitt (2004), Seismic reflection imaging of water mass boundaries in the Norwegian Sea, *Geophys. Res. Lett.*, *31*, L23311, doi:10.1029/2004GL021325.

Nash, J. D., E. Kunze, J. M. Toole, and R. W. Schmitt (2004), Internal tide reflection and turbulent mixing on the continental slope, *J. Phys. Oceanogr.*, *34*, 1117–1134.

Phillips, O. M. (1977), *The Dynamics of the Upper Ocean*, 336 pp., Cambridge Univ. Press, New York.

Polzin, K. L., J. M. Toole, J. R. Ledwell, and W. R. W. R.Schmitt (1997), Spatial variability of turbulent mixing in the abyssal ocean, *Science*, *276*, 93–96.

Proni, J. R., and J. R. Apel (1975), On the use of high-frequency acoustics for the study of internal waves and microstructure, *J. Geophys. Res.*, *80*, 1147–1151.

Rudnick, D. L., et al. (2003), From tides to mixing along the Hawaiian Ridge, *Science*, *301*, 355–357.

Stoughton, R. B., S. M. Flatté, and B. Howe (1986), Acoustic measurements of internal-wave rms displacement and rms horizontal current off bermuda in late 1983, *J. Geophys. Res.*, *91*, 7721–7732.

Thorpe, S. A. (1975), The excitation, dissipation, and interaction of internal waves in the deep ocean, *J. Geophys. Res.*, *80*, 328–338.

Thorpe, S. A. (1987), On the reflection of a train of finite amplitude internal gravity waves from a uniform slope, *J. Fluid Mech.*, *178*, 279–302.

Toole, J. M., K. L. Polzin, and R. W. Schmitt (1994), New estimates of diapycnal mixing in the abyssal ocean, *Science*, *264*, 1120–1123.

Toole, J. M., R. W. Schmitt, K. L. Polzin, and E. Kunze (1997), Near-boundary mixing above the flanks of a mid-latitude seamount, *J. Geophys. Res.*, *102*, 947–959.

Widess, M. (1973), How thin is a thin bed?, *Geophysics*, *38*, 1176–1180.

———————

W. S. Holbrook, Department of Geology and Geophysics, University of Wyoming, Laramie, WY 82071, USA. (steveh@uwyo.edu)

I. Fer, Bjerknes Centre for Climate Research and Geophysical Institute, University of Bergen, N-5007 Bergen, Norway.